Charge fluctuations in the single-electron box: Perturbation expansion in the tunneling conductance

Hermann Grabert
Fakultät für Physik, Albert-Ludwigs-Universität, Hermann-Herder-Straße 3, 79104 Freiburg, Germany
(Received 19 May 1994)

The average number of electrons on a small metallic island biased by an external voltage source via a tunnel junction is investigated. The jumps of the electron number as a function of the applied voltage are smeared by quantum fluctuations arising from the finite tunneling conductance of the junction. A systematic expansion of the partition function in terms of the tunneling conductance is given. The average island charge is determined for the realistic case where the electronic bandwidth is large compared to the single-electron charging energy. It is shown that finite-temperature effects remain important for the lowest temperatures presently attainable experimentally.

I. INTRODUCTION

In recent years, Coulomb blockade phenomena in nanostructured metallic films have attracted a great deal of interest.[1,2] Typically these systems consist of small conductors interrupted by tunnel junctions and gate capacitors for external control. Single-electron effects are observed in these systems provided two basic requirements are met. First, the charge on a small metallic island between two tunnel junctions or between a tunnel junction and a capacitor should be quantized in units of the elementary charge. Second, the Coulomb energy of a single excess electron on an island should surmount the thermal energy k_BT.

The simplest system showing single-electron charging effects is the single-electron box.[3] It consists of an ultrasmall tunnel junction with capacitance C in series with an equally small gate capacitance C_G, where typically $C, C_G < 1$ fF. The device is controlled by an external voltage source U_{ex} (cf. Fig. 1). Provided the tunneling resistance R_t of the junction exceeds the von Klitzing constant $R_K = h/e^2 \sim 25.8\,\mathrm{k\Omega}$, the charge q on the metallic island between the junction and the capacitor is found to be quantized, i.e., $q = -ne$, where n is the number of excess electrons on the island. A simple electrostatic calculation gives for the ground state an electron number n which is the integer closest to $n_{ex} = C_G U_{ex}/e$. Hence, n is a step function of the applied voltage as shown in Fig. 1. By changing U_{ex} electrons can be added one by one to the box in a reversible way.

This simple picture of Coulomb blockade phenomena in the single-electron box is modified by three kinds of effects. First, at finite temperatures excited states are available and the steps will be smeared.[3] Second, the island charge q is not strictly quantized. The coupling between the Fermi liquids in the island and lead electrodes by the tunnel junction allows for a hybridization of their states which gives rise to a quantum smearing of the steps.[4,5] Finally, the external voltage source is attached to the box by leads. The interaction with this electromagnetic environment modifies the simple electrostatic energy considerations.[6] However, in view of an earlier examination,[7] we expect only small environmental effects for standard experimental setups. Hence, we shall focus here on the effect of the finite tunneling conductance and finite temperatures on charge quantization.

In the following section, we first introduce an appropriate Hamiltonian and relate the average number of excess electrons in the box with the partition function of the system. Using the tunneling Hamiltonian as a perturbation, we then derive in Sec. III a series expansion of the partition function. The perturbation theory is complicated by the fact that the Fermi liquids in the island and lead electrodes are correlated by the charging energy. We restrict ourselves to the limit of a large number of electronic channels, which is realistic for metallic tunnel junctions. Sections IV, V, and VI discuss the diagrammatic representation of the perturbation series, which is condensed step by step. Also, we take the limit where the electronic bandwidth is large compared to the single-electron charging energy, as it is the case in real systems. In Sec. VII, we then use the these results to determine the effect of the finite tunneling conductance on the Coloumb staircase. Explicit results are given up to second order in the tunneling conductance. Finally, in Sec. VIII, we present our conclusions.

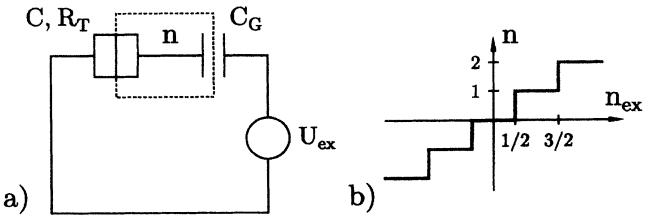

FIG. 1. (a) The circuit diagram of the single-electron box, consisting of a tunnel junction in a series with a capacitor. (b) The number n of electrons in the box as a function of $n_{ex} = C_G U_{ex}/e$.

 ©1994 The American Physical Society

II. HAMILTONIAN AND PARTITION FUNCTION

An appropriate Hamiltonian for the single-electron box may be written as

$$H = H_0 + H_t\,, \tag{1}$$

where

$$H_0 = E_c(n - n_{\rm ex})^2 + \sum_{k\sigma} \epsilon_{k\sigma}\, a^\dagger_{k\sigma}\, a_{k\sigma} + \sum_{q\sigma} \epsilon_{q\sigma}\, a^\dagger_{q\sigma}\, a_{q\sigma} \tag{2}$$

describes the system in the absence of tunneling.

$$E_c = \frac{e^2}{2(C + C_G)} \tag{3}$$

is the single-electron charging energy, and n denotes the number operator of excess electrons on the metallic island between the tunnel junction and the gate capacitance (cf. Fig. 1).

$$n_{\rm ex} = C_G\, U_{\rm ex}/e \tag{4}$$

is a dimensionless parameter characterizing the applied voltage $U_{\rm ex}$. Hence, the first term on the rhs of (2) describes the Coulomb energy in the presence of an external voltage.[3] Hereby we have omitted terms independent of n that are irrelevant for the following considerations.

The remaining terms in (2) describe the Fermi liquids in the island and lead electrodes, respectively. $a_{k\sigma}$ is the annihilation operator of an electron state with energy $\epsilon_{k\sigma}$ in the island electrode. Here, k denotes the longitudinal wave number, and σ denotes the transversal and spin quantum numbers. Likewise, $a_{q\sigma}$ is the annihilation operator of an electron state with energy $\epsilon_{q\sigma}$ in the lead electrode, where q denotes the longitudinal wave number. The transversal wave number and the spin quantum number, both denoted by σ, are conserved during tunneling transitions described by the tunneling Hamiltonian,

$$H_t = \sum_{kq\sigma} (t_{kq\sigma}\, a^\dagger_{k\sigma}\, a_{q\sigma}\, \Lambda + \text{H.c.})\,. \tag{5}$$

Here, $t_{kq\sigma}$ is the transition amplitude for tunneling of an electron from the state $q\sigma$ in the lead electrode to the state $k\sigma$ in the island electrode. The operator Λ changes the number n of excess electrons on the island by 1, i.e.,

$$\Lambda^\dagger n \Lambda = n + 1\,. \tag{6}$$

In terms of the phase φ conjugate to n with the commutation relation

$$[n, \varphi] = i\,, \tag{7}$$

the operator Λ may be written as

$$\Lambda = \exp(-i\varphi)\,. \tag{8}$$

At inverse temperature $\beta = 1/k_B T$, the partition function Z of the single-electron box reads

$$Z = \text{tr}\,\{\exp(-\beta H)\}\,, \tag{9}$$

from where we obtain in terms of the free energy $F = -(1/\beta)\ln Z$

$$\frac{\partial F}{\partial n_{\rm ex}} = \left\langle \frac{\partial H}{\partial n_{\rm ex}} \right\rangle\,, \tag{10}$$

where $\langle\,\rangle$ denotes the thermal average. In view of $\partial H/\partial n_{\rm ex} = -2E_c(n - n_{\rm ex})$ this gives for the average number $\langle n\rangle$ of excess electrons in the box

$$\langle n\rangle = n_{\rm ex} - \frac{1}{2E_c}\frac{\partial F}{\partial n_{\rm ex}} = n_{\rm ex} + \frac{1}{2\beta E_c}\frac{\partial \ln Z}{\partial n_{\rm ex}}\,. \tag{11}$$

Hence, we need to determine the partition function Z as of function of $n_{\rm ex}$ to calculate the average number of charges in the box.

III. PERTURBATION THEORY IN THE TUNNELING HAMILTONIAN

To evaluate the partition function we shall treat the tunneling Hamiltonian H_t as a small perturbation. We first note that due to the charging energy, the Hamiltonian H_0 does not imply a Wick theorem for the expectation values of time ordered products of electron creation and annihilation operators. In this and the following sections, we present direct thermodynamics perturbation techniques for this case.[8]

We first note that the unperturbed Hamiltonian may be written

$$H_0 = H_c + \sum_\sigma H_\sigma\,, \tag{12}$$

where

$$H_c = E_c(n - n_{\rm ex})^2 \tag{13}$$

is the charging energy, and

$$H_\sigma = \sum_k \epsilon_{k\sigma}\, a^\dagger_{k\sigma}\, a_{k\sigma} + \sum_q \epsilon_{q\sigma}\, a^\dagger_{q\sigma}\, a_{q\sigma} \tag{14}$$

is the electronic Hamiltonian for channel σ. Further, the tunneling Hamiltonian is of the form

$$H_t = \sum_\sigma h_\sigma\,, \tag{15}$$

where

$$h_\sigma = t \sum_{kq\zeta} \zeta a^\zeta_{k\sigma}\, a^{-\zeta}_{q\sigma}\, \Lambda^{-\zeta}\,. \tag{16}$$

Here, we have replaced $t_{kq\sigma}$ by a constant and real transition amplitude t, which is sufficient for our purposes. The index ζ takes the two values + and −, and we have introduced the notations $a^+_{p\sigma} = a^\dagger_{p\sigma}$, $a^-_{p\sigma} = a_{p\sigma}$ (p =

$k,q)$, $\Lambda^+ = \Lambda^\dagger$, $\Lambda^- = \Lambda$ for convenience. Note that the various channels σ are coupled by the charging energy H_c.

Since the n_{ex} dependence of the partition function arises from the charging energy only, we may put

$$Z = \frac{\operatorname{tr} e^{-\beta H}}{\Pi_\sigma \operatorname{tr}_\sigma e^{-\beta H_\sigma}} . \tag{17}$$

A straightforward expansion in powers of H_t gives by virtue of (12) and (15)

$$Z = \sum_{m=0}^{\infty} (-1)^m \int_0^\beta d\alpha_m \int_0^{\alpha_m} d\alpha_{m-1} \cdots \int_0^{\alpha_2} d\alpha_1 \sum_{\sigma_1,\ldots,\sigma_m} \frac{\operatorname{tr}_c e^{-\beta H_c} \Pi_\sigma \operatorname{tr}_\sigma e^{-\beta H_\sigma} h_{\sigma_m}(\alpha_m) \cdots h_{\sigma_1}(\alpha_1)}{\Pi_\sigma \operatorname{tr}_\sigma e^{-\beta H_\sigma}} , \tag{18}$$

where tr_c is the trace over all charge states of the box, and tr_σ is the trace over all electron states in channel σ. Furthermore,

$$h_\sigma(\alpha) = e^{\alpha H_0} h_\sigma e^{-\alpha H_0} . \tag{19}$$

Inserting now the representation (16) into (18), and writing the trace over the charge states explicitly, we find

$$Z = \sum_{m=0}^{\infty} (-1)^m \int_0^\beta d\alpha_m \int_0^{\alpha_m} d\alpha_{m-1} \cdots \int_0^{\alpha_2} d\alpha_1 \sum_{k_1 q_1 \sigma_1 \zeta_1} \cdots \sum_{k_m q_m \sigma_m \zeta_m} t^m \zeta_1 \zeta_2 \cdots \zeta_m$$

$$\times \sum_{n=-\infty}^{+\infty} e^{-\sum_{j=1}^m (\alpha_j - \alpha_{j-1}) E_{n_j}} \left\langle a^{\zeta_m}_{k_m \sigma_m}(\alpha_m) a^{-\zeta_m}_{q_m \sigma_m}(\alpha_m) \cdots a^{\zeta_1}_{k_1 \sigma_1}(\alpha_1) a^{-\zeta_1}_{q_1 \sigma_1}(\alpha_1) \right\rangle_0 . \tag{20}$$

Here, $\alpha_0 = \alpha_m - \beta$, and the n_j give the number of charges in intermediate states with

$$n_1 = n, \quad n_j = n + \sum_{k=1}^{j-1} \zeta_k \quad (j > 1). \tag{21}$$

Further,

$$E_n = E_c (n - n_{ex})^2 \tag{22}$$

is the charging energy in the presence of n electrons in the box. Finally,

$$\langle X \rangle_0 = \frac{\Pi_\sigma \operatorname{tr}_\sigma e^{-\beta H_\sigma} X}{\Pi_\sigma \operatorname{tr}_\sigma e^{-\beta H_\sigma}} \tag{23}$$

is a thermal average for a system with Hamiltonian

$$H_0' = \sum_\sigma H_\sigma , \tag{24}$$

that is the unperturbed system in the absence of charging effects. Accordingly, the time-dependent creation and annihilation operators are given by

$$a^\pm_{p\sigma}(\alpha) = e^{\alpha H_\sigma} a^\pm_{p\sigma} e^{-\alpha H_\sigma} \quad (p = k, q) . \tag{25}$$

Since the Hamiltonian H_0' implies a Wick theorem, the expectation values in (20) are readily evaluated. We first note that nonvanishing contributions are only obtained for m even. Furthermore, using cyclic invariance properties of the integrand, (20) may be written as

$$Z = \sum_{m=0}^{\infty} \frac{\beta}{2m} t^{2m} \int_0^\infty d\beta_1 \cdots \int_0^\infty d\beta_{2m} \, \delta\left(\sum_{j=1}^{2m} \beta_j - \beta\right)$$

$$\times \sum_{\zeta_1,\ldots,\zeta_{2m}} \sum_{n=-\infty}^{\infty} e^{-\sum_{j=1}^{2m} \beta_j E_{n_j}}$$

$$\times \sum_{k_1 q_1 \sigma_1} \cdots \sum_{k_{2m} q_{2m} \sigma_{2m}} \left\langle \prod_{j=1}^{2m} \zeta_j \, a^{\zeta_j}_{k_j \sigma_j} \left(\sum_{l=1}^{j} \beta_l\right) \right.$$

$$\left. \times a^{-\zeta_j}_{q_j \sigma_j} \left(\sum_{l=1}^{j} \beta_l\right) \right\rangle_0 . \tag{26}$$

Now, all nonvanishing contractions are of the form

$$\langle a^\zeta_{p_1 \sigma}(\tau_2) a^{-\zeta}_{p_2 \sigma}(\tau_1) \rangle = \delta_{p_1,p_2} \frac{e^{\zeta(\tau_2 - \tau_1)\epsilon_{p\sigma}}}{1 + e^{\zeta\beta\epsilon_{p\sigma}}} \quad (p = k, q) . \tag{27}$$

Hence, only terms with

$$\sum_{j=1}^{2m} \zeta_j = 0 \tag{28}$$

contribute to Z, and each channel index σ_j must occur at least twice for different signs of ζ_j. In metallic tunnel junctions the number of channels

$$N = \sum_\sigma 1 \tag{29}$$

is typically very large. Then terms where four or more channel indices coincide give only corrections at most of

order $1/N$ and may be disregarded.

When evaluating (26) with the help of (27), we encounter products of terms of the form

$$Y(\tau_2-\tau_1) = t^2 \sum_{k_1 q_1 k_2 q_2 \sigma} \langle a^{\zeta}_{k_2\sigma}(\tau_2) a^{-\zeta}_{k_1\sigma}(\tau_1)\rangle_0 \times \langle a^{-\zeta}_{q_2\sigma}(\tau_2) a^{\zeta}_{q_1\sigma}(\tau_1)\rangle_0 = t^2 \sum_{kq\sigma} \frac{e^{\zeta(\tau_2-\tau_1)(\epsilon_{k\sigma}-\epsilon_{q\sigma})}}{(1+e^{\zeta\beta\epsilon_{k\sigma}})(1+e^{-\zeta\beta\epsilon_{q\sigma}})} . \quad (30)$$

Now, the metallic bandwidth D is very large compared with the relevant energy scales E_c and k_BT. Later, we will show that we can take the limit $D/E_c \to \infty$. In intermediate formulas, we keep the bandwidth finite whenever necessary and assume symmetrical bands with exponential cutoff for convenience. Hence, we replace the sums over longitudinal wave numbers by

$$\sum_k F(\epsilon_{k\sigma}) \to \rho \int_{-\infty}^{+\infty} d\epsilon\, e^{-|\epsilon|/D} F(\epsilon) \quad (31)$$

and

$$\sum_q F(\epsilon_{q\sigma}) \to \rho' \int_{-\infty}^{+\infty} d\epsilon\, e^{-|\epsilon|/D} F(\epsilon) , \quad (32)$$

where ρ and ρ' are the densities of states per channel in the island and lead electrodes, respectively. The function (30) then takes the form

$$Y(\tau) = g \int_{-\infty}^{+\infty} d\epsilon\, e^{-|\epsilon|/D} \frac{\epsilon}{1-e^{-\beta\epsilon}} \quad e^{-\tau\epsilon} , \quad (33)$$

where we have introduced the dimensionless parameter

$$g = t^2 N \rho \rho' \quad (34)$$

and have performed one energy integral in the large bandwidth limit. In terms of the usual expression for the tunneling resistance R_t of the junction, the parameter g may be written as

$$g = \frac{1}{4\pi^2} \frac{R_K}{R_t} , \quad (35)$$

where $R_K = h/e^2$ is the von Klitzing constant.

Upon inserting for the δ function in (26) the representation

$$\delta(\alpha) = \frac{1}{2\pi} \int_{-\infty}^{+\infty} dE\, e^{-i\alpha E} \quad (36)$$

and evaluating the expectation values in terms of (30) and (33), the partition function becomes

$$Z = \sum_{m=0}^{\infty} \frac{\beta}{2m} \int_0^{\infty} d\beta_1 \cdots \int_0^{\infty} d\beta_{2m} \frac{1}{2\pi} \int_{-\infty}^{+\infty} dE\, e^{i\beta E} \times \sum_{\zeta_1,\ldots,\zeta_{2m}} \sum_{n=-\infty}^{\infty} e^{-\sum_{j=1}^{2m} \beta_j (E_{n_j}+iE)} \sum_{\text{pairs}} \prod_{k=1}^{m} Y(\tau_k) . \quad (37)$$

In view of (28) there are m positive and negative vertices ζ_j, respectively. The sum over pairs is over the $m!$ connections of + and − vertices in pairs, and

$$\tau_k = \sum_{j=1}^{2m} \beta_j \theta_{jk} , \quad (38)$$

where $\theta_{jk} = 1$ for time intervals β_j in between the two vertices connected, and $\theta_{jk} = 0$ otherwise. Inserting the explicit form (33) of $Y(\tau)$ and (38) into (37), we see that the β_j integrals can be carried out explicitly yielding

$$Z = \sum_{m=0}^{\infty} \frac{1}{2\pi} \int_{-\infty}^{+\infty} dE\, e^{i\beta E} \frac{\beta}{2m} \sum_{n=-\infty}^{+\infty} \sum_{\zeta_1,\cdots,\zeta_{2m}} \times \int_{-\infty}^{+\infty} d\epsilon_1 \frac{g\,\epsilon_1\, e^{-|\epsilon_1|/D}}{1-e^{-\beta\epsilon_1}} \cdots \int_{-\infty}^{+\infty} d\epsilon_m \frac{g\,\epsilon_m\, e^{-|\epsilon_m|/D}}{1-e^{-\beta\epsilon_m}} \times \sum_{\text{pairs}} \prod_{j=1}^{2m} \frac{1}{E_{n_j} + \sum_{k=1}^{m} \theta_{jk}\epsilon_k + iE} . \quad (39)$$

This expansion of Z lends itself to a diagrammatic representation discussed in the following section.

IV. CIRCLE DIAGRAMS FOR THE EXPANSION OF THE PARTITION FUNCTION

The series (39) may be written as a sum over diagrams. For a diagram of order m, we put down a circle with $2m$ points. Each point is a vertex carrying a sign ζ_j. Since in (39) two sequences $\{\zeta_1,\ldots,\zeta_{2m}\}$ of vertices that are cyclic permutations of each other give the same contribution to Z, it is sufficient to put down only *distinct* sequences of signs made up of m + and − signs, respectively. Sequences that can be obtained by cyclic permutation are not distinct. Sequences made up of d identical subsequences have *divisor d*. For instance, the sequence $+-+-+-$ has divisor 3. Weighting a diagram with divisor d by a factor $2m/d$, we regain the full sum over $\zeta_1,\ldots,\zeta_{2m}$ in (39). For each sequence of vertices positive and negative vertices are connected in pairs in all possible ways by tunnelon lines. Microscopically, such a line describes the intermediate formation of a tunnelon excitation, that is the creation of an electron-hole pair where the electron and the hole are on different sides of the junction due to electron tunneling.

Figure 2 shows all diagrams up to second order and some higher order diagrams. The expansion (39) may now be written as

$$Z = \frac{1}{2\pi} \int_{-\infty}^{+\infty} dE\, e^{i\beta E} \sum_{\text{diagrams}} D(E) . \quad (40)$$

A diagram of order m and divisor d contains (i) a factor β/d, (ii) a sum over all charge states $\sum_{n=-\infty}^{+\infty} \cdots$, (iii) an integration $\int_{-\infty}^{+\infty} d\epsilon_k \frac{g\,\epsilon_k\, e^{-|\epsilon_k|/D}}{1-e^{-\beta\epsilon_k}} \cdots$ for each of the m tunnelon lines $(k = 1,2,\ldots,m)$, and (iv) a factor $\left(E_{n_j} + \sum_{k=1}^{m} \theta_{jk}\epsilon_k + iE\right)^{-1}$ for each of the $2m$ seg-

ments of the circle ($j = 1, 2, \ldots, 2m$), where n is the charge quantum number of an arbitrary segment labeled 1. As one goes around the circle, say counterclockwise, the charge quantum number changes at each vertex by ± 1 according to the sign of the vertex. See diagrams (d) and (h) in Fig. 2 for a possible labeling. Finally, $\theta_{jk} = 1$ for the sequence of segments j connecting the vertices of tunnelon line k, and $\theta_{jk} = 0$ for the remaining segments of the circle. Since the contribution of the diagram can be shown to be invariant under the transformation $\theta_{jk} \to 1 - \theta_{jk}$, it does not matter which arc is chosen to connect two vertices.

As a function of the energy E, a diagram $D(E)$ has poles in the complex plane arising from the energy denominators associated with the $2m$ segments. These poles give contributions to the integral in (40). Hence Z may be written as

$$Z = \sum_{\text{diagrams}} 1/d \sum_{\text{segments}} S, \tag{41}$$

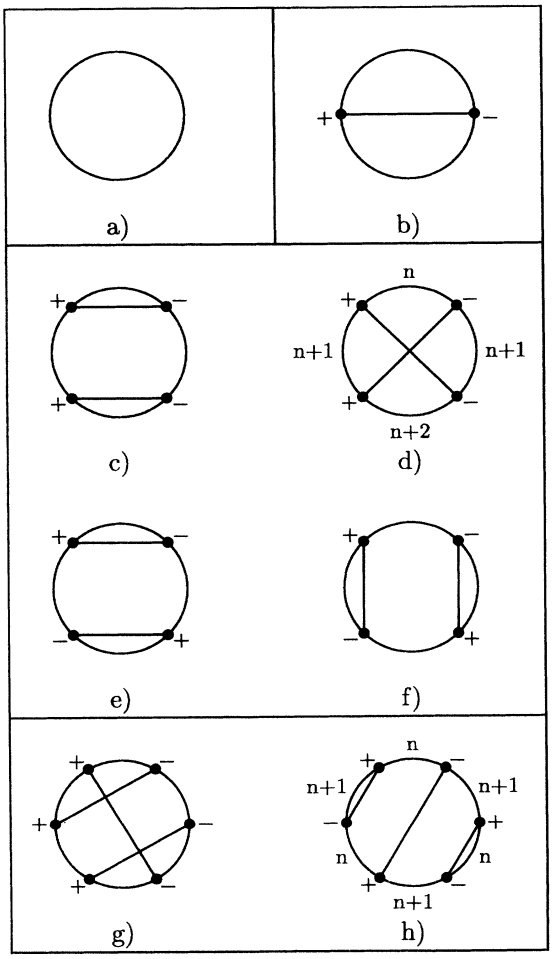

FIG. 2. Diagrams for the partition function. (a) Zeroth-order, (b) first-order, (c)–(f) all second-order, (g) and (h) selected third-order diagrams. Diagrams (e) and (f) have divisor 2, (h) has divisor 3, all others have divisor 1. Charge quantum numbers are shown explicitly for diagrams (d) and (h).

where the sum over segments runs over the $2m$ segments of the circle of a diagram of order m, and S gives the contribution of the pole associated with this segment.

A segment is of *degree* r if by cutting this segment and $(r-1)$ other segments the diagram can be decomposed into r disconnected parts, such that the diagram falls into pieces at each cut following the first cut. For instance, the uppermost segments of diagrams (f) and (h) in Fig. 2 are of degree 2. Going from one of the r cut segments to a neighboring one along the circle, intermediate tunnelon excitations are created and again annihilated, so that the energy denominators associated with these r segments coincide leading to a pole of order r.

The contribution of this pole to the integral (40) is readily evaluated. The r segments of degree r are found to contribute to the sum over segments in (41) the term

$$S_r = \sum_{n=-\infty}^{+\infty} e^{-\beta E_n} \sum_{p=1}^{r} \frac{\beta^p}{(p-1)!\,(r-p)!} \times \left(-\frac{\partial}{\partial E_n}\right)^{r-p} \prod_{q=1}^{r} T_q \,. \tag{42}$$

Here, n is the charge quantum number of the r segments, and the T_q describe the contributions of the r subdiagrams. A subdiagram with $2l$ vertices contains an integration (iii) for each of the l tunnelon lines, and a factor (iv) for each of the $2l-1$ segments, where the n_j and θ_{jk} are defined by the rules given previously.

The expression (42) for S_r contains differential operators with respect to E_n acting upon the $2m-r$ energy denominators, that are associated with the segments of the r subdiagrams T_q. Diagrammatically a differential operator may be represented by decorating the corresponding segment with a slash. We then find

$$S_r = \sum_{s=0}^{r-1} \sum_{\text{decorations}} S_r^{(s)}, \tag{43}$$

where the sum over decorations runs over all possibilities to distribute s slashes among the $2m-r$ segments of the r subdiagrams, including multiple slashes. We consider only diagrams with topologically distinct arrangements of slashes. Then, a diagram where n_p segments are decorated with p slashes must be weighted by a multiplicity factor

$$M(n_p) = s! \prod_{p=0}^{\infty} \frac{1}{(p!)^{n_p}} \tag{44}$$

according to the various sequences possible in putting down the

$$s = \sum_{p=0}^{\infty} p n_p \tag{45}$$

slashes to produce this particular decoration.

Using these rules the contribution S_r of r segments of degree r may be written as

$$S_r = \sum_{s=0}^{r-1} \sum_{\text{decorations}} \sum_{n=-\infty}^{+\infty} e^{-\beta E_n} \frac{\beta^{r-s}}{(r-s-1)!} \prod_{q=1}^{r} T_q \,. \tag{46}$$

For a given decoration the r subdiagrams T_q carry s slashes altogether, and the contribution of a subdiagram T_q with $2l$ vertices contains the usual l integrations for the l tunnelon lines and a factor

$$\Sigma_j = \frac{(-1)^{q_j}}{\left(E_{n_j} + \sum_{k=1}^{l} \theta_{jk}\epsilon_k - E_n\right)^{q_j+1}} \tag{47}$$

for each of the $2l-1$ segments, where q_j is the number of slashes carried by the segment, while E_{n_j} and θ_{jk} are defined as previously. Combining (41) and (46), we obtain the complete diagrammatic expansion of the partition function.

To illustrate the diagrammatic rules let us evaluate the contribution of some of the diagrams depicted in Fig. 2. The zeroth-order diagram (a) gives

$$Z_0 = \sum_{n=-\infty}^{+\infty} e^{-\beta E_n}, \tag{48}$$

and the first order diagram (b) yields

$$Z_1 = \sum_{n=-\infty}^{+\infty} e^{-\beta E_n} \beta g \int_{-\infty}^{+\infty} \frac{d\epsilon\, \epsilon\, e^{-|\epsilon|/D}}{1-e^{-\beta\epsilon}} \times \left\{ \frac{1}{E_{n+1}-E_n+\epsilon} + \frac{1}{E_{n-1}-E_n+\epsilon} \right\}. \tag{49}$$

Note that both segments of this diagram are of degree 1. In this case (46) simplifies to read

$$S_1 = \sum_{n=-\infty}^{+\infty} e^{-\beta E_n} \beta T_1, \tag{50}$$

where T_1 is the subdiagram obtained by omitting the segment in question. For diagram (b) the subdiagram associated with the upper segment consists of the tunnelon line and the lower segment. If the charge quantum number of the upper segment is n, the lower segment carries $n+1$ charges, so that T_1 contains one integration factor from the tunnelon line and one energy denominator $(E_{n+1}+\epsilon-E_n)^{-1}$ from the lower segment yielding the first term in (49). Correspondingly, the second term contains the contribution of the lower segment.

As an example for a second-order contribution to Z, we consider diagram (e) in Fig. 2. This diagram has divisor 2. The upper and the lower segments are of degree 1. Both segments give identical contributions arising from a subdiagram with two tunnelon lines and three segments, where the two outer segments have the same energy denominators. The contribution $Z_2^{(e,1)}$ of the upper and lower segments is found to read

$$Z_2^{(e,1)} = \sum_{n=-\infty}^{+\infty} e^{-\beta E_n} \beta g^2 \int_{-\infty}^{+\infty} \frac{d\epsilon\, \epsilon\, e^{-|\epsilon|/D}}{1-e^{-\beta\epsilon}} \times \int_{-\infty}^{+\infty} \frac{d\epsilon'\, \epsilon'\, e^{-|\epsilon'|/D}}{1-e^{-\beta\epsilon'}} \left(\frac{1}{E_{n+1}-E_n+\epsilon}\right)^2 \times \frac{1}{\epsilon+\epsilon'}. \tag{51}$$

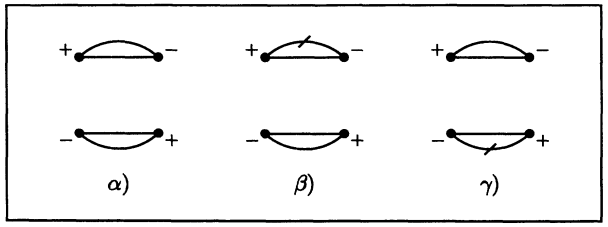

FIG. 3. Decorated subdiagrams describing the contribution of the segments of degree 2 of diagram (e) in Fig. 2.

The segments on the right and left of diagram (e) are of degree 2. According to (46) the subdiagrams have to be decorated with zero or one slash in all possible ways yielding the diagrams depicted in Fig. 3. Their contribution is found to read

$$Z_2^{(e,2)} = \frac{1}{2} \sum_{n=-\infty}^{+\infty} e^{-\beta E_n} \beta g^2 \times \int_{-\infty}^{+\infty} \frac{d\epsilon\, \epsilon\, e^{-|\epsilon|/D}}{1-e^{-\beta\epsilon}} \int_{-\infty}^{+\infty} \frac{d\epsilon'\, \epsilon'\, e^{-|\epsilon'|/D}}{1-e^{-\beta\epsilon'}} \times \left\{ \frac{\beta}{(E_{n-1}-E_n+\epsilon)(E_{n-1}-E_n+\epsilon')} - \frac{2}{(E_{n-1}-E_n+\epsilon)^2(E_{n-1}-E_n+\epsilon')} \right\}, \tag{52}$$

where the first term comes from diagram (α), while the second term comes from diagrams (β) and (γ) that give identical contributions. To proceed it is advantageous to pass from the circle diagrams considered so far to vertical diagrams introduced in the following section.

V. VERTICAL DIAGRAMS AND EFFECTIVE CHARGING ENERGY

In the expansion of the partition function in terms of circle diagrams there is a factor $1/d$ for diagrams with divisor d. Mostly this factor cancels when the contributions of all segments are summed. Consider a circle diagram D with $2m$ vertices and divisor d. Then, the contribution of a segment j ($j = 1, 2, \ldots, 2m$) arises d times, since the segments $j + (2m/d)l$ ($l = 1, 2, \ldots, d-1$) of the diagrams which are similar to D but "turned" by $2\pi l/d$ give the same contribution, except for the case where the turned diagram is identical to D. However, in this latter case the segment $j + (2m/d)l$ of D gives the same contribution as segment j, except for the case where the diagram can be split into two parts by cutting the segments j and $j + (2m/d)l$. Let l_0 be the smallest value of l where the last situation arises. Clearly, D then splits into $f = d/l_0$ identical subdiagrams. The various possibilities discussed here are illustrated in Fig. 4.

So far we have considered circle diagrams that are evaluated segment by segment. To proceed it is advantageous to introduce an alternative type of vertical diagrams that describe directly the contribution of these circle segments. According to (46), the contribution of r segments of degree r is given in terms of r subdiagrams

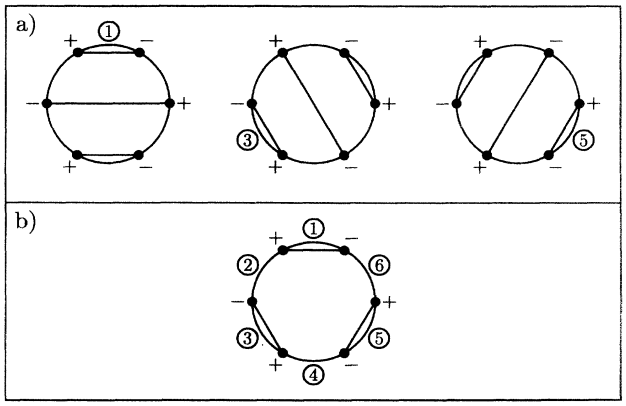

FIG. 4. (a) Three circle diagrams with divisor 3 that are turned by $2\pi/3$ with respect to each other. The three segments labeled explicitly give the same contribution. (b) A circle diagram with divisor 3 that coincides with its versions turned by $\pm 2\pi/3$. The three segments labeled 1, 3, and 5 give the same contribution. The segments 2, 4, and 6 are of degree 3 and the diagram splits into three identical subdiagrams.

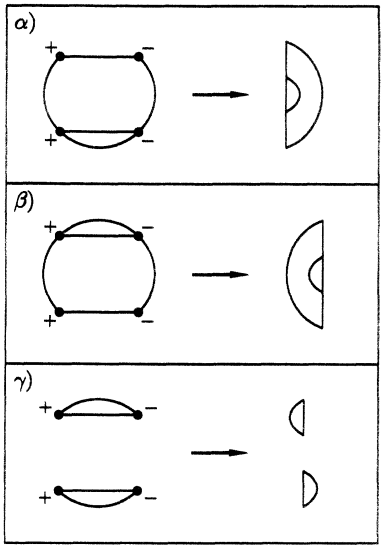

FIG. 5. Subdiagrams for the contributions of the segments of diagram (c) in Fig. 2. To the left (right) the circle (vertical) diagrams are shown. (α) describes the contribution of the upper segment, (β) of the lower segment, and (γ) of the two remaining segments that are of degree 2. Decorations with slashes are not shown.

T_q. Omitting the decoration with slashes for the time being, each subdiagram consists of $2l$ vertices, l tunnelon lines, and $2l-1$ segments. We redraw these subdiagrams in the following way. The arc in the counterclockwise direction is drawn as a descending charge line. The tunnelon lines are drawn as arcs to the right (left) if they start at a positive (negative) vertex. The signs ζ_j of the vertices may then be omitted. An arc curving to the left will also be called the antitunnelon line in the sequel.

By way of example, Fig. 5 shows the subdiagrams describing the contributions of the segments of circle diagram (c) in Fig. 2. Note that in the circle diagrams the charge line is curved and the tunnelon lines are straight, while the opposite is true for the vertical diagrams. The vertical diagrams are generated in the following way. For diagrams of order m we draw a vertical charge line with $2m$ vertices. Then + signs are attached to m vertices and − signs to the remaining vertices in all possible ways. Finally, positive and negative vertices are connected by arcs in all possible ways. An arc or tunnelon (antitunnelon) line where the upper vertex is positive (negative) is drawn to the right (left), so that the vertex signs may be omitted afterwards. A diagram is of degree r, if by cutting the charge line the diagram can be decomposed into r irreducible pieces, where irreducible diagrams are those of degree 1. Diagrams which are cyclic permutations of the same sequence of irreducible subdiagrams are not distinct.

A diagram has *factor* f if it is made up of a sequence of f identical subgroups of irreducible diagrams. Notice, a diagram with factor f is of degree $r = f \cdot l$, where l is an integer. Now, the r irreducible subdiagrams of a diagram of degree r have $2m - r$ charge line segments altogether, that must be decorated with s ($s = 0, 1, 2, \ldots, r-1$) slashes in all possible ways. In terms of this set of decorated vertical diagrams the expansion (41), (46) of the partition function may be rewritten as

$$Z = \sum_{\text{diagrams}}^{\text{cp}} \sum_{n=-\infty}^{+\infty} e^{-\beta E_n} \times \sum_{s=0}^{r-1} \frac{\beta^{r-1}}{(r-s-1)!} \frac{1}{f} \left[\prod_{q=1}^{r} T_q \right]^{(s)} , \tag{53}$$

where the first sum is over all vertical diagrams. The index cp indicates that cyclic permutations of the r irreducible subdiagrams T_q of a diagram of degree r are not distinct. The symbol $[\ldots]^{(s)}$ stands for the sum over all decorations of the diagrams between the brackets with s slashes. According to the considerations at the beginning of this section, the factor $1/d$ in (41) is replaced by $1/f$ in (53), where f is the factor of the diagram. The contribution of an irreducible subdiagram T_q with $2l$ vertices is given by

$$T_q(E) = \int_{-\infty}^{+\infty} \frac{d\epsilon_1\, g\epsilon_1\, e^{-|\epsilon_1|/D}}{1 - e^{-\beta\epsilon_1}} \cdots \int_{-\infty}^{+\infty} \frac{d\epsilon_l\, g\epsilon_l\, e^{-|\epsilon_l|/D}}{1 - e^{-\beta\epsilon_l}} \times \prod_{j=1}^{2l-1} \frac{(-1)^{q_j}}{(E_{n_j} - E_n + \sum_{k=1}^{l} \theta_{jk}\, \epsilon_k + E)^{q_j+1}} , \tag{54}$$

that is an integration for each (anti-) tunnelon line k ($k = 1, 2, \ldots, l$) and a factor of the form (47) for each charge line segment j ($j = 1, 2, \ldots, 2l-1$), where q_j is the number of slashes carried by the segment. Numbering the segments from above, we have $n_1 = n \pm 1$ depending on the sign of the uppermost vertex, and n_j changes by ± 1 at each vertex according to its sign as one descents the charge line. The $\theta_{jk} = 1$ if the (anti-) tunnelon line k passes to the right or left of segment j, and $\theta_{jk} = 0$ oth-

erwise. For later purposes, we have introduced in (54) an additional variable E. Of course, in (53) we have to insert the expression (54) for $E = 0$.

Since a diagram of degree r and factor f has r/f cyclic permutations, we may distinguish cyclic permutations of irreducible subdiagrams and replace the factor $1/f$ in (53) by $1/r$ instead. Then, introducing the quantities

$$U_r^{(s)}(E) = \sum_{\text{diagrams}} \left[\prod_{q=1}^{r} T_q(E)\right]^{(s)} , \tag{55}$$

where the sum is over all diagrams of degree r with cyclic permutations of the irreducible subdiagrams T_q now being distinguished, the partition function (53) may be written as

$$Z = \sum_{n=-\infty}^{+\infty} e^{-\beta E_n} \left\{1 + \sum_{p=1}^{\infty} \frac{\beta^p}{p!} \sum_{s=0}^{\infty} \frac{p}{p+s} U_{p+s}^{(s)}(0)\right\} . \tag{56}$$

Note that the $U_r^{(s)}(E)$ depend on the charge quantum number n. This index will be suppressed temporarily in order not to overload the formulas.

Now, introducing

$$I(E) = \sum_{\text{diagrams}} T(E) , \tag{57}$$

which is the sum over all irreducible diagrams without slashes and coincides with $U_1^{(0)}(E)$, we have

$$(\partial/\partial E)^s I(E) = s! \sum_{\text{diagrams}} [T(E)]^{(s)} . \tag{58}$$

This is because a differential operator $\partial/\partial E$ acting upon the sum over all irreducible diagrams with $s-1$ slashes generates each diagram with s slashes exactly s times, since any of these s slashes may be the one added last. Hence, we find

$$U_1^{(s)}(E) = \frac{1}{s!} \frac{\partial^s I(E)}{\partial E^s} . \tag{59}$$

Further, $U_r^{(s)}(E)$ may be written as

$$U_r^{(s)}(E) = \sum_{\{n_p\}} \frac{r!}{\prod_{p=0}^{s} n_p!} \prod_{p=0}^{s} \left[U_1^{(p)}(E)\right]^{n_p} , \tag{60}$$

where the sum is over all sequences $\{n_p\}$, $n_p = 0, 1, 2, \ldots$, with

$$\sum_{p=0}^{s} n_p = r , \quad \sum_{p=0}^{s} p n_p = s . \tag{61}$$

This is because $U_r^{(s)}(E)$ is the sum over all products of r irreducible diagrams carrying s slashes altogether. Distributing these slashes among the r factors in all possible ways, we obtain (60) where the numerical factor arises, since permutations of the irreducible diagrams are distinguished in the sum over diagrams in (55). Inserting (59) into (60), we obtain

$$U_r^{(s)}(E) = \frac{1}{s!} \frac{\partial^s I^r(E)}{\partial E^s} . \tag{62}$$

Furthermore, in view of the relation

$$\left(\sum_{s=0}^{\infty} \frac{1}{(s+1)!} \frac{\partial^s I^{s+1}(E)}{\partial E^s}\right)^p = \sum_{s=0}^{\infty} \frac{p}{p+s} \frac{1}{s!} \frac{\partial^s I^{p+s}(E)}{\partial E^s} , \tag{63}$$

which follows from Lagrange's theorem,[9] we have

$$\sum_{s=0}^{\infty} \frac{p}{p+s} U_{p+s}^{(s)}(E) = \left(\sum_{s=0}^{\infty} \frac{1}{s+1} U_{s+1}^{(s)}(E)\right)^p , \tag{64}$$

so that the partition function (56) may be written as

$$Z = \sum_{n=-\infty}^{+\infty} e^{-\beta(E_n + \Delta_n)} , \tag{65}$$

where

$$\begin{aligned} \Delta_n &= -\sum_{s=0}^{\infty} \frac{1}{s+1} U_{s+1}^{(s)}(0) \\ &= -\sum_{\text{diagrams}} \sum_{s=0}^{\infty} \frac{1}{s+1} \left[\prod_{q=1}^{s+1} T_q\right]_n^{(s)} . \end{aligned} \tag{66}$$

Here, the irreducible subdiagrams T_q have to be evaluated according to (54) with $E = 0$, and we have made their dependence on the charge quantum number n explicit. Clearly,

$$E_n^{\text{eff}} = E_n + \Delta_n \tag{67}$$

may be viewed as an effective charging energy of the island in the presence of n excess electrons. Apart from n and n_{ex}, the correction Δ_n arising from electron tunneling depends on the tunneling resistance and on temperature. The diagrammatic expansion (66) may be represented in a more convenient form presented in the following section.

VI. DIAGRAMS WITH INSERTIONS AND INFINITE BANDWIDTH LIMIT

According to (66) the effective energy shift Δ_n is the sum over all diagrams of degree $s+1$ ($s = 0, 1, 2, \ldots,$) carrying s slashes. Since permutations of the subdiagrams are distinguished in this sum, each set of decorated subdiagrams occurs $(s+1)!$ times. Now, a given set of $s+1$ irreducible diagrams decorated with s slashes altogether may be combined into a single diagram by inserting other subdiagrams at the positions of the slashes. This assembling of a single diagram with insertions can be made in $s!$ ways. In terms of these diagrams the result (66) may simply be written as

$$\Delta_n = \sum_{\text{diagrams}} U_n \,, \tag{68}$$

since the factors $(s+1)!$ and $1/s!$ from the permutations and the assembling, respectively, cancel the factor $1/(s+1)$ in (67). Now, the perturbative expansion of the effective energy shift Δ_n may be written as

$$\Delta_n = \sum_{m=1}^{\infty} \Delta_n^{(m)} \,, \tag{69}$$

where $\Delta_n^{(m)}$ is the sum of diagrams of order m.

The diagrams U of order m are obtained by drawing a vertical charge line with $2m$ points and connecting pairs by tunnelon lines that curve to the right or antitunnelon lines that curve to the left in all possible ways. Diagrams that can be separated into two disconnected parts by cutting the charge line have to be excluded. In addition, one has to draw all possible diagrams having one or several insertions, including insertions into insertions. The beginning and the end of an insertion is marked as a prolongation of the tunnelon line across the vertical charge line. Each insertion has to be an allowed lower order diagram and the same must be true for the diagram remaining if the insertion is removed.

All first-order and second-order diagrams, as well as some third-order diagrams are shown in Fig. 6. A diagram U_n with index n and without insertions is evaluated in the following way. Each vertical line segment represents a charge state, that may be labeled by the number of excess electrons in the box. At the upper end one starts out with n excess electrons, and each tunnelon (antitunnelon) excitation increases (decreases) the charge quantum number by 1. Now, U_n contains an integration

$$g \int_{-\infty}^{+\infty} \frac{d\epsilon\, \epsilon\, e^{-|\epsilon|/D}}{1-e^{-\beta\epsilon}} \cdots$$

for each (anti-) tunnelon line, and an energy factor $-1/E$ for each charge line segment, where E is the excitation energy, that is the sum of the charging energy and the energies ϵ of the (anti-) tunnelons present in the intermediate state minus the initial energy E_n. Note that there is an odd number of charge line segments giving rise to the $-$ sign in (66). Accordingly, the contribution of the first-order diagrams in Fig. 6(a) reads

$$\Delta_n^{(1)} = -g \int_{-\infty}^{+\infty} \frac{d\epsilon\, \epsilon\, e^{-|\epsilon|/D}}{1-e^{-\beta\epsilon}} \left(\frac{1}{E_{n+1}-E_n+\epsilon} + \frac{1}{E_{n-1}-E_n+\epsilon} \right). \tag{70}$$

Likewise, the first second-order diagram in Fig. 6(b) gives

$$\Delta_n^{(2,1)} = -g^2 \int_{-\infty}^{+\infty} d\epsilon_1 \int_{-\infty}^{+\infty} d\epsilon_2 \frac{\epsilon_1\, \epsilon_2\, e^{-(|\epsilon_1|+|\epsilon_2|)/D}}{(1-e^{-\beta\epsilon_1})(1-e^{-\beta\epsilon_2})} \times \frac{1}{(E_{n+1}-E_n+\epsilon_1)^2\,(E_{n+2}-E_n+\epsilon_1+\epsilon_2)} \,. \tag{71}$$

A diagram U_n with insertions is evaluated in the following way. The inserted part of a diagram is evaluated exactly like the corresponding lower order diagram. The contribution of the rest of the diagram is evaluated with the rules given above. Note that, due to the insertion, the intermediate state above and below the insertion occurs twice. Finally, there is a factor -1 for each insertion. For instance, the ninth diagram in Fig. 6(b) gives the contribution

$$\Delta_n^{(2,9)} = g^2 \int_{-\infty}^{+\infty} d\epsilon_1 \int_{-\infty}^{+\infty} d\epsilon_2 \frac{\epsilon_1\, \epsilon_2\, e^{-(|\epsilon_1|+|\epsilon_2|)/D}}{(1-e^{-\beta\epsilon_1})(1-e^{-\beta\epsilon_2})} \times \frac{1}{(E_{n+1}-E_n+\epsilon_1)^2\,(E_{n+1}-E_n+\epsilon_2)} \,, \tag{72}$$

and all other diagrams in Fig. 6(b) are evaluated accordingly.

Let us investigate the first-order energy shift $\Delta_n^{(1)}$ in greater detail. The result (70) may be written as

$$\Delta_n^{(1)} = -2g \int_{-\infty}^{+\infty} \frac{d\epsilon\, e^{-|\epsilon|/D}}{1-e^{-\beta\epsilon}} \frac{\epsilon}{E_c+\epsilon} + \tilde{\Delta}_n^{(1)} \,, \tag{73}$$

where

$$\tilde{\Delta}_n^{(1)} = g \int_{-\infty}^{+\infty} \frac{d\epsilon\, \epsilon}{1-e^{-\beta\epsilon}} \left(\frac{2}{E_c+\epsilon} - \frac{1}{E_{n+1}-E_n+\epsilon} - \frac{1}{E_{n-1}-E_n+\epsilon} \right). \tag{74}$$

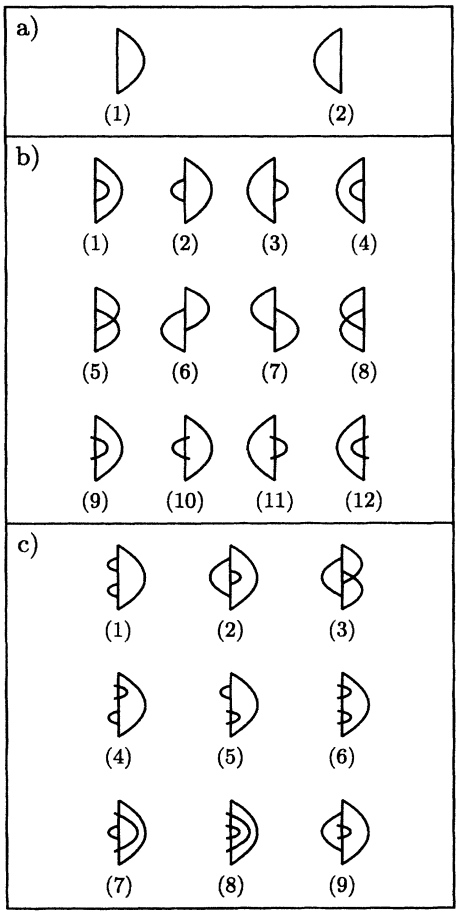

FIG. 6. (a) All first- and (b) all second-order diagrams for the effective energy shift. (c) Some third-order diagrams.

In this last expression, we have taken the infinite bandwidth limit $D/E_c \to \infty$. We note that the first term on the right-hand side of (73) diverges in the infinite bandwidth limit, yet, this term is independent of n and n_{ex}. Hence, it leads to a factor in the partition function (65) that does not contribute to the average number of electrons (11) in the box. Consequently, we may discard this term and replace $\Delta_n^{(1)}$ by $\tilde{\Delta}_n^{(1)}$. Because of

$$E_{n+1} + E_{n-1} - 2E_n = 2E_c\,, \tag{75}$$

the integral (74) converges for $\epsilon \to \infty$, so that $\tilde{\Delta}_n^{(1)}$ is well defined in the infinite bandwidth limit. In practice, D/E_c is very large and this limit is appropriate to the system under consideration.

To determine the second-order energy shift $\Delta_n^{(2)}$, we have to sum the contributions of the twelve diagrams in Fig. 6(b), two of which are given explicitly in (71) and (72). Using the relation (75) and

$$E_{n\pm2} - 2E_{n\pm1} + E_n = 2E_c\,, \tag{76}$$

we obtain after some algebra in the infinite bandwidth limit,

$$\Delta_n^{(2)} = 2g^2 E_c \int_{-\infty}^{+\infty} \frac{d\epsilon_1\,\epsilon_1}{1-e^{-\beta\epsilon_1}} \int_{-\infty}^{+\infty} \frac{d\epsilon_2\,\epsilon_2}{1-e^{-\beta\epsilon_2}} \times \left(\frac{(E_{n-1}-E_{n+1})(\epsilon_1+\epsilon_2) - (E_{n+2}-E_n)(E_{n+1}-E_n+\epsilon_2)}{(E_{n+1}-E_n+\epsilon_1)^2(E_{n+1}-E_n+\epsilon_2)(E_{n-1}-E_n+\epsilon_2)(E_{n+2}-E_n+\epsilon_1+\epsilon_2)(\epsilon_1+\epsilon_2)} + \text{c.t.} \right), \tag{77}$$

where c.t. stands for the same term as the preceeding one with $E_{n\pm p}$ replaced by $E_{n\mp p}$. The integral (77) is found to converge for large ϵ_1 and ϵ_2, so that the limit $D/E_c \to \infty$ is well behaved. Note that each single diagram of Fig. 6(b) diverges in the infinite bandwidth limit, while the sum of all second-order diagrams remains finite.

One can show that this remains true for higher order corrections. To see the convergence of the integrals over tunnelon energies, it is sufficient to consider the zero temperature limit. We first note that for $E_c = 0$, the sum of all diagrams of a given order $m \geq 2$ is exactly zero. This is due to the fact that for $E_c = 0$ the Hamiltonian H_0 implies a Wick theorem and standard many-body perturbation theory can be applied. However, when the diagrams are redrawn as Goldstone diagrams, they are found to consist of m unlinked parts with one loop each. In the absence of charging effects these unlinked diagrams cancel. There are of course further Goldstone diagrams that are connected to a higher degree, but they have less than m loops. Since the channel index σ is conserved along each loop, the contribution of these diagrams is not of order g^m, but at most of order g^m/N, and they may be disregarded when the number of channels $N \gg 1$. Now, in the case $E_c \neq 0$ the Fermi liquids are correlated, and the sum of all diagrams of given order $m \geq 2$ is nonvanishing. On the other hand, the high energy behavior of the diagrams is independent of E_c and temperature. Hence, the sum of all diagrams of a given order remains finite in the infinite bandwidth limit and the factors $\exp(-\,|\,\epsilon\,|\,/D)$ may be omitted.

VII. EXPANSION FOR THE AVERAGE NUMBER OF ELECTRONS IN THE BOX

The charging energy depends on the applied voltage U_{ex} via the dimensionless parameter n_{ex} introduced in (4). This dependence will be made explicit, henceforth. We first note that (22) implies

$$E_n(n_{ex}) = E_{n+1}(n_{ex}+1) = E_{-n}(-n_{ex}). \tag{78}$$

Furthermore, the n_{ex} dependence of the effective energy shifts $\Delta_n^{(m)}$ arises through energy differences of the form

$$E_{n\pm p}(n_{ex}) - E_n(n_{ex}) = E_c\,[p^2 \pm 2p(n-n_{ex})]\,. \tag{79}$$

Hence, the shift in order m may be written as

$$\Delta_n^{(m)}(n_{ex}) = g^m E_c f_m(n-n_{ex}), \tag{80}$$

where the $f_m(u)$ are dimensionless functions of u and the dimensionless inverse temperature βE_c. Since under the sum over diagrams tunnelon and antitunnelon lines may be exchanged, we have $f_m(-u) = f_m(u)$, and the relations (78) remain valid for the effective charging energy $E_n(n_{ex}) + \Delta_n(n_{ex})$. Hence, the partition function (65) has the symmetries

$$Z(n_{ex}) = Z(n_{ex}+1) = Z(-n_{ex})\,, \tag{81}$$

and it is sufficient to consider the interval $0 \leq n_{ex} \leq \frac{1}{2}$.

A. First-order term

Let us first consider the leading order effect of the tunneling conductance for small g. From (74) and (80), we find

$$f_1(u) = -8u^2 \int_{-\infty}^{\infty} dx\, \frac{x}{1-e^{-\beta E_c x}} \times \frac{1}{(1+x)\,[(1+x)^2-4u^2]}\,. \tag{82}$$

Now, at finite temperatures the excitation energies of intermediate states may be negative, and the integral in (82) must be regularized. Since the integrand has poles at $x=-1$ and $x=-1\pm 2u$, the integral must be defined by the principal part which coincides with the average of the two contour integrals shown in Fig. 7. Collecting the contributions of the poles at $x_k = i(2\pi/\beta E_c)k$ ($k = \pm1, \pm2, \ldots$), we obtain

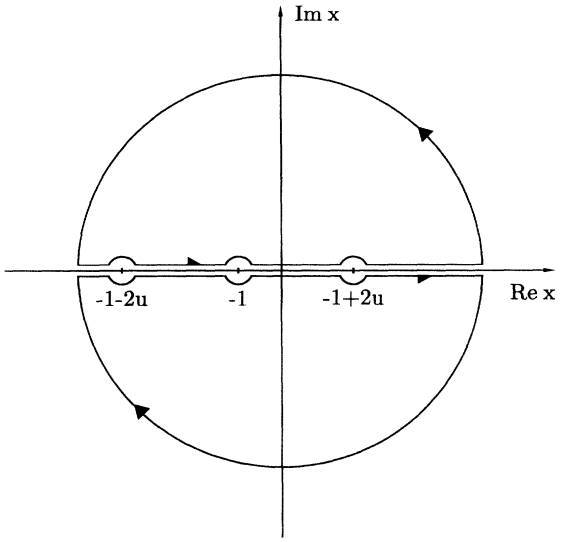

FIG. 7. Integration contours leading from (82) to (83).

$$f_1(u) = 4u^2\nu^2 \sum_{k=-\infty}^{\infty} \frac{|k|}{(1+i\nu k)\left[(1+i\nu k)^2 - 4u^2\right]}, \quad (83)$$

where

$$\nu = \frac{2\pi}{\beta E_c}. \quad (84)$$

The sum in (83) can be evaluated to yield

$$f_1(u) = (1+2u)\mathrm{Re}\left\{\psi(1+i/\nu) - \psi[1+i(1+2u)/\nu]\right\} + (1-2u)\mathrm{Re}\left\{\psi(1+i/\nu) - \psi[1+i(1-2u)/\nu]\right\}, \quad (85)$$

where $\psi(z)$ is the digamma function.

Here, we are mainly interested in the low temperature limit where $\nu \ll 1$. Provided $|1 \pm 2u| \gg \nu$, we obtain from (85)

$$f_1(u) = -(1+2u)\ln|1+2u| - (1-2u)\ln|1-2u| - \frac{2}{3}\frac{u^2}{1-4u^2}\nu^2 + O(\nu^4). \quad (86)$$

In the low temperature limit and in the basic interval $0 \le n_{ex} \le \frac{1}{2}$ only the states $n = 0$ and $n = 1$ contribute appreciably to the partition function (65). For these states, $u = n - n_{ex}$ approaches $\pm\frac{1}{2}$ for $n_{ex} \to \frac{1}{2}$ and the expansion (86) cannot be used in this limit. Since $f_1(u)$ is an even function, it suffices to investigate the behavior near $u = \frac{1}{2}$. For $\nu \ll 1$, we find

$$f_1(u) = -(1+2u)\ln(1+2u) + \frac{1}{3}\frac{u(1+u)}{1+2u}\nu^2 - (1-2u)\left[\mathrm{Re}\left\{\psi[1+i(1-2u)/\nu]\right\} + \ln\nu - \frac{\nu^2}{12}\right] + O(\nu^4), \quad (87)$$

which remains valid for $u = \frac{1}{2}$. In particular, we have $f_1(\frac{1}{2}) = -2\ln 2 + \nu^2/8 + O(\nu^4)$, and the derivative is found to read

$$f_1'(\tfrac{1}{2}) = -2\left[1 + \gamma + \ln(2/\nu)\right] + \nu^2/24 + O(\nu^4), \quad (88)$$

where $\gamma = 0.577\cdots$ is Euler's constant. Note that the derivative diverges logarithmically for $\nu \to 0$. We shall see that this leads to a breakdown of the perturbative expansion near $n_{ex} = \frac{1}{2}$ and $T = 0$.

Now, in the basic interval $0 \le n_{ex} \le \frac{1}{2}$ and for low temperatures the partition function (65) simplifies to read

$$Z(n_{ex}) = P_0(n_{ex}) + P_1(n_{ex}), \quad (89)$$

where

$$P_0(n_{ex}) = \exp\left\{-\beta E_c\left[n_{ex}^2 + g f_1(n_{ex}) + O(g^2)\right]\right\} \quad (90)$$

and

$$P_1(n_{ex}) = P_0(1 - n_{ex}). \quad (91)$$

From (11) and (89)–(91), we readily obtain for the average number of excess electrons in the box

$$\langle n\rangle = -\frac{1}{2}\frac{g f_1'(n_{ex})P_0(n_{ex}) - [2 + g f_1'(1-n_{ex})]P_0(1-n_{ex})}{P_0(n_{ex}) + P_0(1-n_{ex})}. \quad (92)$$

For n_{ex} below $\frac{1}{2} - \frac{1}{\beta E_c}$, we have $P_0(1-n_{ex}) \ll P_0(n_{ex})$, and (92) gives

$$\langle n\rangle = -\tfrac{1}{2} g f_1'(n_{ex}) = g\left[\ln\left(\frac{1+2n_{ex}}{1-2n_{ex}}\right) + \frac{2}{3}\frac{n_{ex}}{(1-4n_{ex}^2)^2}\nu^2 + O(\nu^4)\right]. \quad (93)$$

On the other hand, for $n_{ex} \sim \frac{1}{2}$, we find

$$\langle n\rangle = \tfrac{1}{2} + \chi\varepsilon + O(\varepsilon^2), \quad (94)$$

where $\varepsilon = n_{ex} - \frac{1}{2}$, and

$$\chi = \tfrac{1}{2}\beta E_c + g\left[\beta E_c f_1'(\tfrac{1}{2}) - \tfrac{1}{2} f_1''(\tfrac{1}{2})\right] + O(g^2), \quad (95)$$

is the slope of the Coulomb staircase at the center of the step. Here, $f_1'(\frac{1}{2})$ has been introduced in (88) while $f_1''(\frac{1}{2}) = -2 - \nu^2/12 + O(\nu^4)$. In (95), the small dimensionless tunneling conductance g is multiplied by $f_1'(\frac{1}{2})$, which diverges logarithmically for $T \to 0$. Therefore, as mentioned above, the perturbative expansion breaks down at $T = 0$ near the center of the step. In experiments $k_B T/E_c$ is at least of order 10^{-2}, so that $|\ln \nu|$ remains of order 1. Hence, logarithmically divergent terms near $n_{ex} = \frac{1}{2}$ and $T = 0$ do not cause problems for finite order perturbative results of practical interest.

B. Second-order term

Let us briefly discuss the next order correction. From (77) and (80), we obtain

$$f_2(u) = g_2(u) + g_2(-u)\,, \tag{96}$$

where

$$g_2(u) = 8 \int_{-\infty}^{\infty} dx\, \frac{x}{1 - e^{-\beta E_c x}} \int_{-\infty}^{\infty} dy\, \frac{y}{1 - e^{-\beta E_c y}} \times \frac{u(x+y) - (1-u)(1-2u+y)}{(x+y)(1-2u+x)^2(1-2u+y)(1+2u+y)[4(1-u)+x+y]}\,. \tag{97}$$

These integrals must again be regularized. From an evaluation by contour integration we obtain

$$\begin{aligned} g_2(u) = {} & 2\nu^4 \sum_{\substack{k,l=-\infty \\ k+l\neq 0}}^{+\infty} \frac{|k\,l|\,[i\nu(k+l)\,u - (1-2u+i\nu l)\,(1-u)]}{i\nu(k+l)(1-2u+i\nu k)^2(1-2u+i\nu l)(1+2u+i\nu l)[4(1-u)+i\nu(k+l)]} \\ & -\frac{\pi\nu^3}{2} \sum_{k=-\infty}^{+\infty} \frac{k^2}{(1-2u+i\nu k)^2(1+2u-i\nu k)} + \frac{\nu^4}{8(1-u)} \sum_{k=-\infty}^{+\infty} \frac{k^2}{(1-2u+i\nu k)^2(1-2u-i\nu k)} \\ & +\frac{\nu^4}{4} \sum_{k=-\infty}^{+\infty} \frac{k^2}{(1-2u+i\nu k)^2(1+2u-i\nu k)} + \frac{\nu^4}{2} \sum_{k=-\infty}^{+\infty} \frac{k^2}{(1-2u+i\nu k)^3(1+2u-i\nu k)}\,. \end{aligned} \tag{98}$$

In general, these sums must be evaluated numerically. However, at $T = 0$, the sums in (98) reduce to integrals and we find

$$\begin{aligned} g_2(u) = {} & \frac{\pi^2}{6}(1+2u+8u^2) - \left(\frac{5}{2} - 4u + 2u^2\right) \ln^2\left(\frac{1-2u}{4(1-u)}\right) \\ & +\left(\frac{1}{4} + u + u^2\right) \ln^2\left(\frac{1-2u}{1+2u}\right) + (1+2u) \ln\left(\frac{1-2u}{1+2u}\right) \\ & -4(1-u) \ln\left(\frac{1-2u}{4(1-u)}\right) - (5 - 8u + 4u^2)\,\mathrm{Li}_2\left(\frac{3-2u}{4(1-u)}\right), \end{aligned} \tag{99}$$

where $\mathrm{Li}_2(u) = -\int_0^u dz\, \ln(1-z)/z$ is the dilogarithm function. Using (96) and (99), we obtain for the average number of excess electrons in the box at zero temperature[5]

$$\begin{aligned} \langle n \rangle &= -\tfrac{1}{2}\left[g f_1'(n_{ex}) + g^2 f_2'(n_{ex}) + O(g^3)\right] \\ &= g \ln\left(\frac{1+2n_{ex}}{1-2n_{ex}}\right) + g^2\left[c_2(n_{ex}) - c_2(-n_{ex})\right] + O(g^3)\,, \end{aligned} \tag{100}$$

where

$$\begin{aligned} c_2(u) = {} & -u\left[\frac{4\pi^2}{3} + \ln^2\left(\frac{1-2u}{1+2u}\right)\right] - \frac{16(1+2u-2u^2)}{(3-2u)(1+2u)} \ln(1-2u) \\ & -2(1-u)\left[\ln^2\left(\frac{1-2u}{4(1-u)}\right) + 2\,\mathrm{Li}_2\left(\frac{3-2u}{4(1-u)}\right) - \frac{8(1-u)}{(1-2u)(3-2u)} \ln\left[4(1-u)\right]\right]. \end{aligned} \tag{101}$$

Close to the step finite-temperature effects become important. To second order in g the low temperature partition function is given by (89) and (91) with

$$P_0(n_{ex}) = \exp\Big\{-\beta E_c\,[\,n_{ex}^2 + g f_1(n_{ex}) + g^2 f_2(n_{ex}) + O(g^3)]\Big\}. \quad (102)$$

Evaluating (85) and (96) with (98) numerically, we readily obtain from (102) and (91) the low temperature partition function (89) as a function of n_{ex}. The average number of excess electrons in the box then follows by virtue of (11). Figure 8 shows the resulting form of the Coulomb staircase for various values of R_t/R_K. The curves for $R_t/R_K = \infty$ show the smearing of the staircase function solely due to thermal fluctuations. Clearly, for tunneling resistances of the order of R_K or smaller, quantum charge fluctuations give a significant contribution to the broadening of the step already for $\beta E_c = 10$. For $\beta E_c = 100$ the zero-point charge fluctuations dominate except for voltages very close to the center of the step where finite-temperature effects remain important. This becomes apparent from Fig. 8(c), where various approximations are compared for a relatively large tunneling conductance. The first-order and second-order approximations differ only little. This indicates that the explicit second-order results given above should be sufficient for most practical purposes. The zero temperature result shown in Fig. 8(c) includes a resummation of the most divergent logarithmic terms near $n_{ex} = \frac{1}{2}$. The resummation ensures that the correct value $\langle n\rangle = \frac{1}{2}$ for $n_{ex} = \frac{1}{2}$ is approached.[4,5] Except for the region near the center of the step, the zero temperature result is given by Eq. (100), which gives a reasonable approximation for the low temperature charge fluctuations in this voltage range.

VIII. CONCLUSIONS

In summary, we have calculated the average charge on a voltage biased small metallic island for the realistic case of an electronic bandwidth D that is large compared to the single-electron charging energy E_c. It was shown that for temperatures and tunneling resistances that are typical for current experimental setups the effect of charge fluctuations on the Coulomb blockade effect can be calculated by means of a finite order perturbation expansion in the tunneling conductance. A more sophisticated treatment is only necessary at $T = 0$. On the basis of the present approach, the zero temperature behavior was already discussed in an earlier paper.[5] The extended theory presented here includes finite-temperature effects.

Our work is distinguished from other attempts[4,10–13] by two main features. First, we do not truncate the problem to an effective two-state system. Second, we eliminate the electronic cutoff by taking the infinite bandwidth limit which is well behaved in our approach. While a two-state approximation suffices to extract the low temperature behavior, one has to introduce cutoff dependent effective parameters. In contrast, we give results explicitly in terms of the charging energy and the tunneling conductance measurable at high temperatures in the classical regime. This is essential for a detailed comparison with experimental data. Moreover, we have shown that finite-temperature effects are still important at the low-

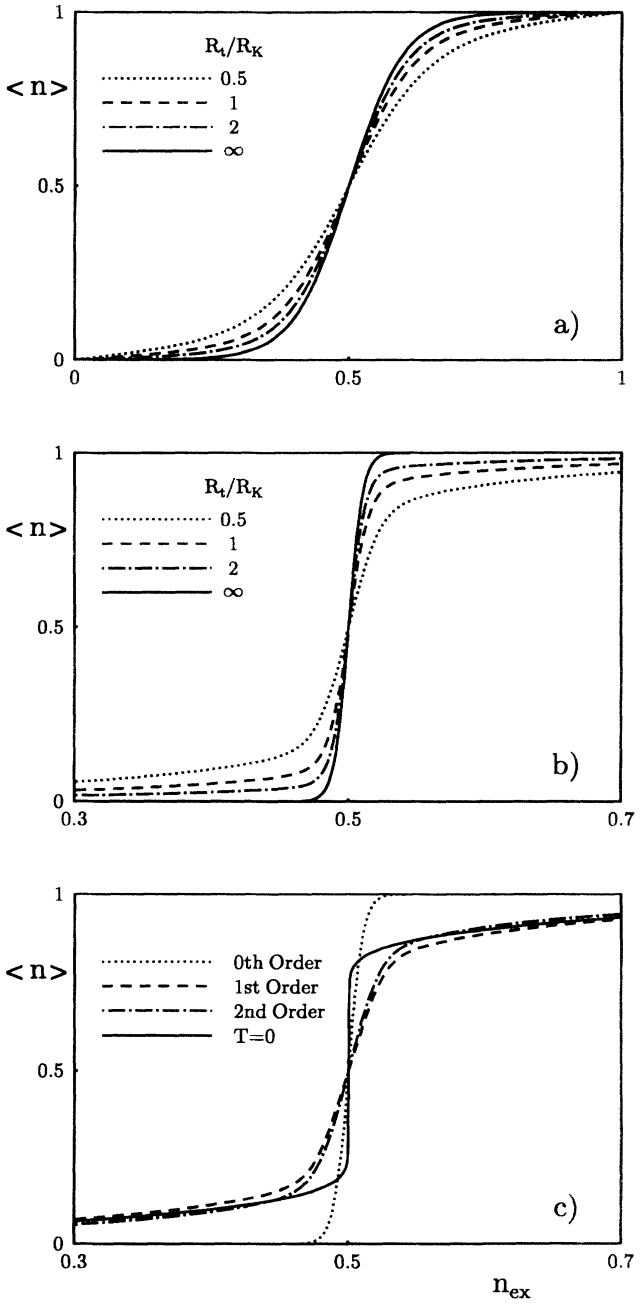

FIG. 8. (a) Average electron number $\langle n\rangle$ of the single-electron box as a function for the applied voltage in dimensionless units n_{ex} for $k_BT = 0.1\ E_c$ and various values of R_t/R_K. (b) Same quantity for $k_BT = 0.01E_c$. (c) A comparison of various approximations for $k_BT = 0.01E_c$ and $R_t = 0.5R_K$.

est temperatures presently attainable experimentally, in particular, near the center of the step.

Finite-temperature results are also of substantial interest for scanning tunneling microscope (STM) systems showing Coulomb staircase patterns.[14,15] In these systems a tunnel junction is formed between the tip of a STM and an ultrasmall metallic particle isolated from the substrate by an oxide barrier. Interestingly, under appropriate conditions Coulomb charging effects may be observed even at room temperature.[16] Setups where the resistance of the particle-substrate junction is much larger than the resistance of the particle-STM-tip junction are feasible. The metallic grain then behaves like the island of an electron box, where the tunneling conductance can be modified by moving the tip. This system may be well suited to test the theoretical predictions made here.

Finally, our results demonstrate that for tunneling resistances of the order of R_K or larger the assumption of a quantization of island charges made in standard theoretical treatments of Coulomb blockade phenomena[1,2] is very reasonable. On the other hand, the deviations from a strict charge quantization should be large enough to allow for a detailed experimental investigation of the effect of the finite tunneling conductance on the average charge in the single-electron box.

ACKNOWLEDGMENTS

The author would like to thank M. H. Devoret, D. Esteve, G.-L. Ingold, P. Lafarge, and P. Riseborough for valuable discussions. The help by F. Neumann and F.-J. Weiper with the figures is gratefully acknowledged. Financial support was provided by the Deutsche Forschungsgemeinschaft (Bonn) through SFB237, by the European Community under Contract No. SC1*-CT91-0631, and by NATO under Grant No. CRG 930115.

[1] *Single Charge Tunneling, Coulomb Blockade Phenomena in Nanostructures*, Vol. 294 of *NATO Advanced Study Institute, Series B: Physics*, edited by H. Grabert and M. H. Devoret (Plenum, New York, 1992).

[2] D. V. Averin and K. K. Likharev, in *Mesoscopic Phenomena in Solids*, edited by B. Altshuler *et al.* (Elsevier, Amsterdam, 1991).

[3] P. Lafarge, H. Pothier, E. R. Williams, D. Esteve, C. Urbina, and M. H. Devoret, Z. Phys. B **85**, 327 (1991).

[4] K. A. Matveev, Zh. Eksp. Teor. Fiz. **99**, 1598 (1991); [Sov. Phys. JETP **72**, 892 (1991)].

[5] H. Grabert, Physica **194-196B**, 1011 (1994).

[6] H. Grabert, G.-L. Ingold, M. H. Devoret, D. Esteve, H. Pothier, and C. Urbina, Z. Phys. B **84**, 143 (1991); G.-L. Ingold and Yu. V. Nazarov, in *Single Charge Tunneling, Coulomb Blockade Phenomena in Nanostructures* (Ref. 1).

[7] H. Grabert and G.-L. Ingold, in *Computations for the Nano-Scale*, Vol. 240 of *NATO Advanced Study Institute, Series E: Applied Physics*, edited by P. E. Blöchl *et al.* (Kluwer, Dordrecht, 1993).

[8] For related methods see, e.g., H. Keiter and G. Morandi, Phys. Rep. **109**, 227 (1984).

[9] See, e.g., E. T. Whittaker and G. N. Watson, *A Course of Modern Analysis* (Cambridge, New York, 1927), p. 132.

[10] S. V. Panyukov and A. D. Zaikin, Phys. Rev. Lett. **67**, 3168 (1991).

[11] G. Falci, G. Schön, and G. T. Zimanyi (unpublished).

[12] D. S. Golubev and A. D. Zaikin (unpublished).

[13] H. Schoeller (private communication).

[14] P. J. M. van Bentum, R. T. M. Smokers, and H. van Kempen, Phys. Rev. Lett. **60**, 2543 (1988).

[15] R. Wilkins, E. Ben-Jacob, and R. C. Jaklevic, Phys. Rev. Lett. **63**, 801 (1989).

[16] C. Schönenberger, H. van Houten, and H. C. Donkersloot, Europhys. Lett. **20**, 249 (1992).